RAMReS Sciences des Structures et de la Matière Vol. 8, N°1 (2024) 1 - 8
http://publication.lecames.org/index.php/mat ISSN: 2630-1180

Cassava vascular bacteriosis detection using spectral measurement of color leaf

Bagui K. Olivier[1,*], Kouakou K. Constant[1,2], Yebouet A. Florence[1], Kouacou Abaka[1], J.T. Zoueu[1]

[1]*Laboratoire Instrumentation Image et Spectroscopie : Département du génie électrique et électronique, Institut National Polytechnique, Yamoussoukro, Côte d'Ivoire*
[2]*Laboratoire de Physique Fondamentale et Appliquée : Unité de Formation et de Recherche des Sciences Fondamentales et Appliquées, Université Nangui Abrogoua, Abidjan, Côte d'Ivoire*

Received: 6 November 2023 / Received in revised form: 16 February 2024 / Accepted: 8 March 2024

***Abstract*:**

Cassava constitutes one of the main priority crops identified by the Ivorian government in the National Strategy for the Development of Food Crops (SNDCV). However, this plant is subject to bacterial attacks which considerably impact production. Early detection of pathologies created by these bacterial infections is therefore essential to determine appropriate treatment. Traditional identification methods take time and sometimes diseases appear before identifying the pathology. The aim of this work is to propose an automatic method for the early detection of one of the pathologies which is cassava vascular bacteriosis. The method we propose uses the L*a*b* color space, obtained from leaf reflectance spectra, defined by the International Commission on Illumination, obtained from the reflectance spectra of the leaves. These characteristic elements are used to establish a learning model using artificial neural networks. The results obtained from the model show perfect detection of vascular bacteriosis of cassava with regard to the coefficient R-square = 0.98 and RMSE = 0.05 and confirm the potential of this approach in making decisions on the state of health of the plant.

***Keywords*:** Cassava vascular bacteriosis ; Reflectance spectra ; L*a*b* ; Neural network.

1 Introduction

Cassava is the second most important food crop in Ivory Coast. Cassava culture supports economic activities and helps to decrease poverty in our country [1]. However, cassava production is limited by many biotic constraints [2, 3]. Major disease that affects cassava plant is vascular bacteriosis (CBB for Cassava Bacterial Blight) caused by *Xanthomonas axonopodis pv. manihotis* (Xam) [4, 5, 6]. In cassava plant, disease can be found on leaves. It is one of the crucial causes that reduces quantity and degrades quality of cassava products up to 80% [7] depending on the

*Correspondant author:
Email address: *kossan.bagui@inphb.ci (O.K. Bagui)*

variety, the stage of the plant and the environment. Therefore, early stage detection is necessary to prevent production loss and ensure the quality of cuttings for future crops.

Traditionally cassava farmers identify the diseases by naked eye observing the presence of disease spot on the leaves. Also, experts identification is based on the experimental result by culturing pathogens in the laboratory [8]. Drawbacks of these methods are that visual assessment is a subjective and no-accurate approach. While culturing pathogens in the laboratory is a time consuming process and there is no guarantee to provide the result on time [8]. Both conventional approaches require experts to identify diseases and it is difficult for farmers to have access to experts [9]. So, a fast and accurate approach to identify vascular bacteriosis is needed.

Some researchers have used different color spaces to develop processing techniques for automatic detection and classification of plant diseases. These automatic systems can help and guide farmers to decide and choose the right pesticides at the right time. Nowadays, many diseases of agricultural plants have been identified, differentiated using automatic systems based on colorimetric spaces [10, 11].

In this work, we proposed a mathematical model for automatic detection of cassava vascular bacteriosis using artificial neural networks (ANN). We use a color space defined by the International Commission on Illumination (CIE) referred to L*a*b*(L* for perceptual lightness and a* and b* for the four unique colors of human vision: red, green, blue and yellow). These three parameters are used as characteristics for establishing the prediction model.

An Artificial Neural Network (ANN) is an information processing paradigm that is inspired by the way biological nervous systems, such as the brain, process the information. It is composed of a large number of highly interconnected processing elements (neurons), they share information from one to another [12-14]. ANNs, like people, automatically generate features from the learning material that they process and solve problems.

2 Materials and Methods

2.1 Sample preparation

The experiment was carried out in boxes of dimension 2×2×1.5 cubic meters. Boxes were covered with mosquito nets on the northern site of the National Polytechnic Institute Houphouët Boigny (INP-HB) of Yamoussoukro in Ivory Coast located at an altitude of 229 m, geographical coordinates 06°53'17.5''N and 05°13'19.6''W. Cassava plants were grown in 15 liter pots containing a mixture of organic soil and sand (3:1 v/v) due to three plants per pot. These pots were spaced 1.5 meters apart. Plants were watered as needed to maintain soil water content (about 55–85%). Relative humidity was 80% conducive to disease.

Fig. 1. Experimental plan.

Forty-five-day-old plants were inoculated with a strain (*Xanthomonas axonopodis pv. manihotis Xam*) by infiltration as described in [15]. From a syringe containing a bacterial suspension calibrated at an optical density (OD) of 0.2 at a wavelength of 600 nm, corresponding to 108 bacteria/mL. The bacterium isolate was obtained by collecting symptomatic leaves in fields near INP-HB. The bacterium was cultured on solid LPGA (Levure Peptone Glucose Agar) medium prepared as follows: yeast 7 g, peptone 7 g, glucose 7 g, Agar-agar 18 g, plus 1000 ml of distilled water at pH = 7.2 for 28 °C. Altogether, we had thirty-six healthy plants and thirty-six infected plants.

2.2 Spectral measurement

The acquisition system consists of four main components: a white LED light source (400-700 nm), a microcontroller (arduino), a spectrometer (USB 4000, Ocean optics) with a spectral range of 350-1050 nm and a computer. The figure 2 presents the experimental setup. Measurements were made on mature leaves of inoculated plants and healthy plants. The L*a*b* colorimetric space was obtained from the reflectance spectra according to the method described by [16].

3 Results and Discussion

Figure 3 shows the images of healthy (a) and infected (b) leaves. For the infected plants, we notice the diseases spots on some leaves. These spots attest the presence of bacteriosis. We carried out the measurements 216 cassava leaves: 108 healthy leaves and 108 infected leaves (on the leaves showing no sign of infection: asymptomatic leaves).

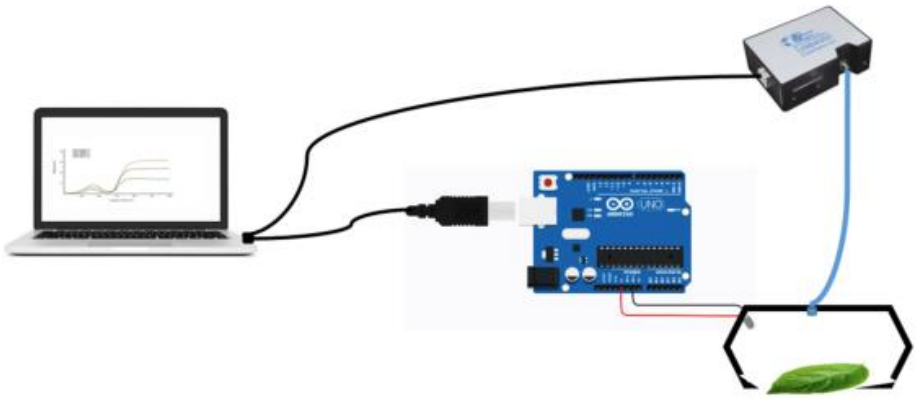

Fig. 2. Experimental setup.

(a) (b)

Fig. 3. Images of healthy plant (a) and infected plant (b).

We registered 216 spectra from the 216 cassava leaves. The healthy leaves spectra are blue and the inoculated leaves spectra are red (see Fig. 4).

The appearance of the spectrum does not make it possible to differentiate healthy leaves from asymptomatic infected leaves. This is due to the fact that the reflectance curve defines energy rate re-emitted in relation to the energy rate received. The two types of leaves present identical colors, which imply a similarity of reflectance curves. Therefore, we extracted the L*a*b* color parameters from these reflectance spectra to verify if a differentiation is possible between the two types of leaves. A simple projection in the L*a*b* space allows us to visualize the trend. Figure 5 presents the result obtained. In this figure, we notice a significant difference between healthy and infected plants. Indeed, the CIELAB chromatic space has the advantage of colors distribution more in line with the perception of color deviations by the human visual system unlike other color spaces. It is particularly used for surface colors characterization. Therefore, we can use this color space to set up a learning model for automatic infection detection.

Before processing the data (neural network application), we divided it into two sets: one to train the model, and the other one to validate the model. The validation set has no effect on training and therefore provides an independent measure of network performance during and after training. It represents 25% of the data and the 75% is attributed to the training set. Subsequently, this training set was divided into three sub-sets: a test, a validation and a training, with a respective percentage of 15%, 15% and 70% [17].

The evaluation of the neural network model performance is highly dependent on the distribution of samples in the data set.

Training data are presented to the network during training and the network is adjusted for its error.

Validation data are used to measure the generalization of the network, and to stop training when the generalization stops improving.

Test data has no effect on training and therefore provides an independent measure of network performance during and after training.

The developed prediction model uses two neurons, a two-layer feed-forward network, with a hyperbolic tangent (tanh) transfer function in the hidden layer and a linear transfer function in the output layer. The activation function which combines the functions of the hidden layer and that of the output layer is described by the Equation (1):

$$Output = LW \times \tanh(IW \times input + B1) + B2 \quad (1)$$

Where:

- Output is a vector which predicts plant health.

$$\text{If Output} = \begin{cases} [1\ 0] & \text{healthy plant} \\ [0\ 1] & \text{infected plant} \end{cases}$$

- Input is a vector which represents the input parameters (L*, a*, b*).
- IW is a [2 3] matrix which contains the weight of the connections between the input layer and the hidden layer.
- LW is a [2 2] matrix which contains the weight of the connections between the hidden layer and the output layer.
- B1 is a vector [2 1] which contains the bias of the input layer.
- B2 is a vector [2 1] which contains the bias of the output layer.

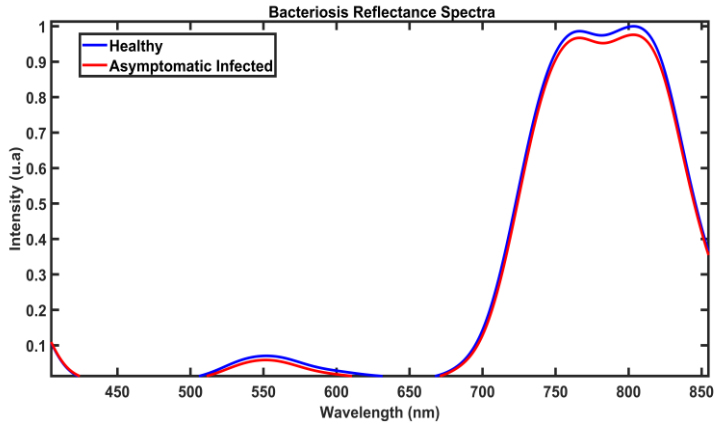

Fig. 4. Reflectance spectra of healthy (blue) and asymptomatic infected leaves (red).

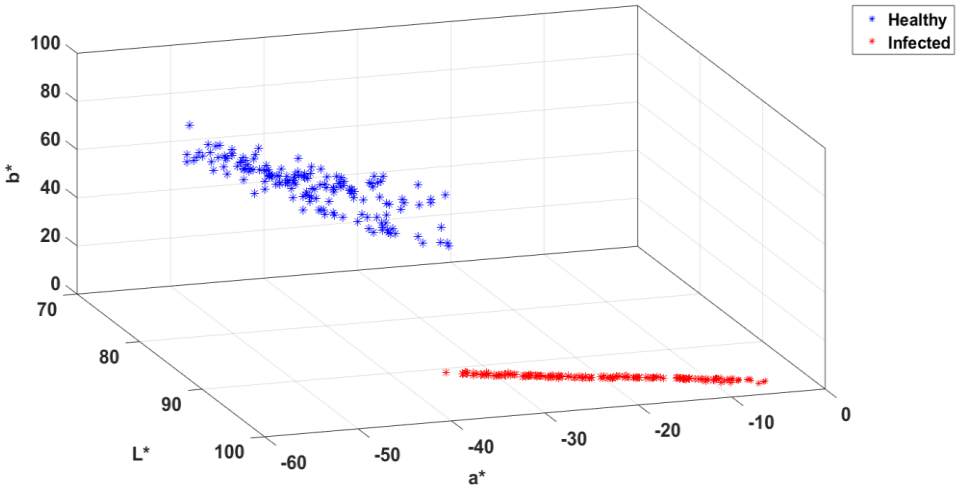

Fig. 5. L*a*b* parameters of healthy (blue *) and asymptomatic infected leaves (red *).

The output is finally obtained by the Equation (2) as follow:

$$\mathbf{Output} = \begin{bmatrix} \mathbf{LW_{11}} & \mathbf{LW_{12}} \\ \mathbf{LW_{21}} & \mathbf{LW_{22}} \end{bmatrix} \times \mathbf{tanh}\left(\begin{bmatrix} \mathbf{IW_{11}} & \mathbf{IW_{12}} & \mathbf{IW_{13}} \\ \mathbf{IW_{21}} & \mathbf{IW_{22}} & \mathbf{IW_{23}} \end{bmatrix} \times \begin{bmatrix} \mathbf{L^*} \\ \mathbf{a^*} \\ \mathbf{b^*} \end{bmatrix} + \begin{bmatrix} \mathbf{B1_{11}} \\ \mathbf{B1_{21}} \end{bmatrix} \right) + \begin{bmatrix} \mathbf{B2_{11}} \\ \mathbf{B2_{21}} \end{bmatrix} \quad (2)$$

The values of LW, IW, B1 and B2 are presented in tables 1 to 4, respectively.

Table 1
LW values.

Matrix components	Values
$\mathbf{LW_{11}}$	-1.92
$\mathbf{LW_{12}}$	-2.92
$\mathbf{LW_{21}}$	1.92
$\mathbf{LW_{22}}$	2.92

Table 2
IW values.

Matrix components	Values
$\mathbf{IW_{11}}$	-10.65
$\mathbf{IW_{12}}$	-51.42
$\mathbf{IW_{13}}$	4.63
$\mathbf{IW_{21}}$	6.89
$\mathbf{IW_{22}}$	54.63
$\mathbf{IW_{23}}$	-3.99

Table 3
B1 values.

Vector components	Values
$\mathbf{B1_{11}}$	2.92
$\mathbf{B1_{21}}$	3.50

Table 4
B2 values.

Vector components	Values
$\mathbf{B2_{11}}$	3.50
$\mathbf{B2_{21}}$	-1.23e-06

To analyze the network response, we examine the confusion matrix by considering the outputs of the trained network and comparing them to the expected results (targets). Figure 6 shows the confusion matrix.

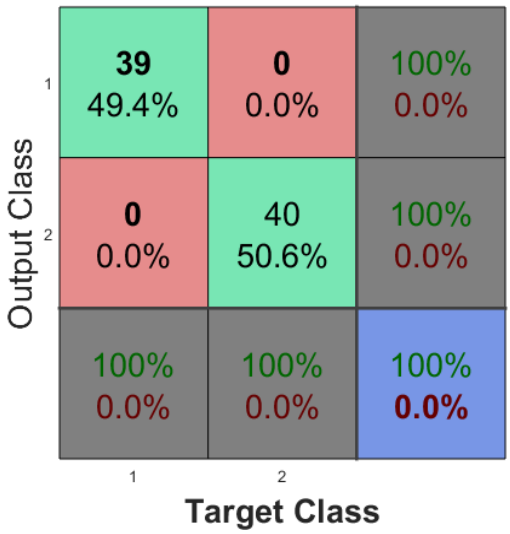

Fig. 6. Confusion matrix.

The diagonal cells show the number of residue positions that were correctly classified for each structural class. The off-diagonal cells show the number of residue positions that were misclassified. The blue cell shows the total percentage of correctly predicted residues and the total percentage of incorrectly predicted residues.

We can deduce from the confusion matrix that our model did excellent learning.
In the following table 5, we calculate the basic indicators of prediction quality to confirm the result of the confusion matrix.

Table 5
Performance indicator.

Performance indicator	Values
R-square	0.9863
RMSE	0.05797

The prediction model quality is evaluated on the basis of the root mean square error (RMSE) and the coefficient of determination (R-square). The RMSE is a measure of the differences between the predicted values by the model and the observed values. The RMSE value is 0.05797; a very low value indicating that the model is good. The coefficient of determination indicates the correlation between predicted infection state and observed infection state. The coefficient R^2 = 98%, a value that tends towards 100%; this shows that the model has indeed ranked the majority of plants. Therefore, it is an efficient model.
The plant confusion matrix shows the responses of the model after being tested. The number of correct answers (True Positive = 49.4% and True Negative = 50.6%) is high compared to the incorrect answers number (False Positive = 0% and False Negative = 0%). This shows that the plants classification by the model corresponds exactly to the state of infection and therefore our model is reliable.

4 Conclusion

Detection of cassava bacterial wilt is a difficult task when visual information of the infection does not appear on the leaves appearance. We have developed a mathematical model for the early detection of cassava bacteriosis. This proposed model is based on CIELAB parameters extraction from reflectance spectra. This approach is simple and can significantly support in recognizing this pathology, thus allowing quick and effective action for the plants treatment.

Funding

We would like to thank the International Science Programme (ISP) and The World Academy of Sciences (TWAS) for financial support.

References

[1] E.R. Krabi, A.A. Assamoi, A.F. Ehon, B. Diawara, L.S. Niamké, T. Philippe, *Production d'attiéké (couscous à base de manioc fermenté) dans la ville d'abidjan*, European Scientific Journal 11(15) (2015) 1857-7881. https://eujournal.org/index.php/esj/article/view/5630

[2] V.N. Fondong, J.S. Pita, M.R. Rey, A. De Kochko, R.N. Beachy, C. Fauquet et al., *Evidence of synergism between African cassava mosaic virus and a new double-recombinant geminivirus infecting cassava in Cameroon*, Journal of General Virology 81 (2000) 287–297. DOI: 10.1099/0022-1317-81-1-287

[3] N.M. Mahungu, K.W. Tata Hangy, S.M. Bidiaka, A. Frangoie, Multiplication de materiel de plantation de manioc et gestion des maladies et ravageurs. Manuel de formation destiné aux agents de terrain, Institut International d'Agriculture Tropicale, RDC (2014).

[4] Piengtawan Tappiban, Supajit Sraphet, Nattaya Srisawad, Duncan R. Smith, Kanokporn Triwitayakorn, *Identification and expression of genes in response to cassava bacterial blight infection*, J. Appl. Genetics 59 (2018) 391–403. https://doi.org/10.1007/s13353-018-0457-2

[5] J. Mansfield, S. Genin, S. Magori, V. Citovsky, M. Sriariyanum, P. Ronald et al., *Top 10 plant pathogenic bacteria in molecular plant pathology*, Molecular Plant Pathology 13 (2012) 614–629.

[6] Carlos A. Zárate-Chaves, Diana Gómez de la Cruz, Valérie Verdier, Camilo E. López, Adriana Bernal, Boris Szurek, *Cassava diseases caused by Xanthomonas phaseoli pv. manihotis and Xanthomonas cassava,* Mol. Plant Pathol. 22(12) (2021) 1520–1537. doi: 10.1111/mpp.13094

[7] S. Restrepo, C.M. Vélez, V. Verdier., *Measuring the Genetic Diversity of Xanthomonas axonopodis pv. manihotis Within Different Fields in Colombia Phytopathologyn*, The American Phytopathological Society 90 (2000) 683 - 690. https://doi.org/10.1094/PHYTO.2000.90.7.683

[8] J.G.A Barbedo, *A review on the Main challenges in automatic plant disease identification based on visible range images*, Biosys.t Eng. 144 (2016) 52–60. https://doi.org/10.1016/j.biosystemseng.2016.01.017

[9] Vimal K. Shrivastava, Monoj K. Pradhan, *Rice plant disease classification*

using color features: a machine learning paradigm, Journal of Plant Pathology 103 (2020) 17–26. https://doi.org/10.1007/s42161-020-00683-3

[10] T. Verma, S. Dubey, *Impact of color spaces and feature sets in automated plant diseases classifier: a comprehensive review based on rice plant images*, Arch. Comput. T. and Methods Eng. 27 (2020) 1611–1632.

[11] S. Nain, N. Mittal, M. Hanmandlu, *CNN-based plant disease recognition using colour space models*, International Journal of Image and Data Fusion (2024) 1–14. https://doi.org/10.1080/19479832.2023.2300335

[12] O.I. Abiodun, A. Jantan, A.E. Omolara, K.V. Dada, N.A. Mohamed, H. Arshad, *State-of-the-art in artificial neural network applications: A survey*, Heliyon 4(11) (2018) e00938. https://doi.org/10.1016/j.heliyon.2018.e00938

[13] Ayman S. El-Baz, Jasjit Suri, State of the Art in Neural Networks and Their Applications, Volume 1, 1st Edition, ISBN: 9780128197400 (2021).

[14] M. Shoaib, B. Shah, S. EI-Sappagh, A. Ali, A. Ullah, F. Alenezi, T. Gechev, T. Hussain, F. Ali, *An advanced deep learning models-based plant disease detection: A review of recent research*, Front. Plant Sci. 14 (2023) 1158933. doi: 10.3389/fpls.2023.1158933

[15] D. Meyer, E. Lauber, D. Roby, M. Arlat, T. Kroj, *Optimization of pathogenity assays to study the Arabidopsis thaliana–Xanthomonas campestris pv. campestris pathosystem*, Molecular Plant Pathology 6 (2005) 327–33. https://doi.org/10.1111/j.1364-3703.2005.00287.x.

[16] https://www.youtube.com/watch?v = LVHbaDs5yVw

[17] Purvanshparmar, Optimal data division for training Neural Network, May 10, 2021. https://purvansh.medium.com/optimal-data-division-for-training-neural-network3c83726e9551